The Chara plasma membrane system : an ancestral model for plasma membrane transport in plant cells

Zhang, S.

Citation

Zhang, S. (2018, May 9). *The Chara plasma membrane system : an ancestral model for plasma membrane transport in plant cells*. Retrieved from https://hdl.handle.net/1887/64136

Author: Zhang, S.
Title: The Chara plasma membrane system : an ancestral model for plasma membrane transport in plant cells
Issue Date: 2018-05-09

Chapter 4

Auxin effects on ion transport in *Chara corallina*

Suyun Zhang[1], Albertus H. de Boer[2], Bert van Duijn[1,3]

[1] Plant Biodynamics Laboratory, Institute of Biology Leiden, Leiden University, Sylvius Laboratory, Sylviusweg 72, 2333 BE Leiden, The Netherlands

[2] Department of Structural Biology, Faculty Earth and Life Sciences, Vrije Universiteit, 1081 HV Amsterdam, The Netherlands.

[3] Fytagoras BV, Sylviusweg 72, 2333 BE Leiden, The Netherlands

Published: Journal of Plant Physiology,193, (2016): 37-44.

Doi: 10.1016/j.jplph.2016.02.009.

Abstract

The plant hormone auxin has been widely studied with regard to synthesis, transport, signaling and functions among the land plants while there is still a lack of knowledge about the possible role for auxin regulation mechanisms in algae with “plant-like” structures. Here we use the alga *Chara corallina* as a model to study aspects of auxin signaling. In this respect we measured auxin on membrane potential changes and different ion fluxes (K^+, H^+) through the plasma membrane. Results showed that auxin, mainly IAA, could hyperpolarize the membrane potential of *C. corallina* internodal cells. Ion flux measurements showed that the auxin-induced membrane potential change may be based on the change of K^+ permeability and/or channel activity rather than through the activation of proton pumps as known in land plants.

Introduction

The plant hormone auxin, IAA, plays an essential role in plant growth and development. With respect to the physiological aspects of this plant hormone we can distinguish the (polar) auxin transport related processes and the (cellular) signaling related processes. Compared to our knowledge of auxin action in (red, brown, green) algae species, the regulation, signaling and working mechanism of auxin is much clearer for the land plant species (Lau et al., 2009; Wright and Nemhauser, 2015; Enders and Strader, 2015; Di et al., 2015). In land plants, auxin is produced in apical parts of the plants and is transported to specific directions with the help of different auxin transporters among which the so-called PIN efflux transporters (Morris, 2000; Viaene et al., 2013; Adamowski and Friml,2015; Qin and Dong, 2015). At the cellular level, active auxin levels can also be regulated by biosynthesis, storage and conjugation with other molecules (Vernoux et al., 2010; Kramer and Ackelsberg, 2015). Research into auxin related cellular signaling showed different physiological responses of plant cells upon auxin stimulation (Berleth et al., 2004). In these responses membrane hyperpolarization, activation of the plasma membrane H^+-ATPases and potassium channels are well established (Ephritikhine et al., 1982; Felle et al., 1991; Van Duijn and Heimovaara-Dijkstra, 1994; Philippar et al., 2004; Christian et al., 2006; Takahashi et al., 2012; Xu et al., 2012; Osakabe et al., 2013).

As it was already shown in the 1950s or even earlier, that algae species naturally synthesize auxin and that the growth of most of marine/fresh water, unicellular/multicellular algae can be regulated by auxin, (van Overbeek, 1940; Cooke et al., 2002; Tarakhovskaya et al., 2007) it is believed that auxin, as an important growth regulator, dates back to a very early stage of plant evolution. Despite these findings basic knowledge of the role, transport and cellular signaling of auxin in algae is very limited. With respect to polar auxin transport (PAT), as a unique aspect of auxin's role in plant growth and development, it is known that in higher plants the responsible auxin carriers can be divided into two groups, auxin-uptake carriers and auxin-efflux carriers. The carriers can be easily distinguished by their different sensitivities to different inhibitors such as NPA (1-N-naphthylphthalamic acid), a specific PAT inhibitor. In algae these auxin transport or carrier systems may be present as well (Dibb-Fuller and Morris, 1992; De Smet et al., 2011; Boot et al., 2012; Feraru et al., 2012). Some evolutionary less developed plants share similar body structures as the higher land plants, suggesting that auxin- like polar transport and gradients may play a role in the development and growth. Indeed, in mosses the existence of polar auxin transport was reported (Fujita and Hasebe, 2009; Viaene et al., 2014), as well as in the cells of the multicellular algae *Chara coralline* (Boot et al., 2012). As a multicellular green alga, *Chara* has a differentiated plant body-like structure, which is also thought to be one of the closest relatives to the land plants (Qiu and Palmer, 1999; Wodniok et al., 2011; Timme et al., 2012; Zhang and van Duijn, 2014). Understanding the role, transport and physiology of auxin in these algae may reveal the evolution of auxin signaling and its functioning in plant evolution. In addition, this may indicate to us yet unknown aspects of auxin in higher plants. It is understandable that with the development of a differentiated, multicellular plant body, a better regulated auxin transmembrane transport pathway is needed to facilitate the morphogenic-signal function of auxin. Based on the studies up to date, there are still debates on whether *Chara* has similar influx and/or efflux auxin transporters, and whether these transporters have similar inhibition sites binding to phototropins. Although polar auxin transport is well established for *Chara* cells it does not automatically imply that auxin acts as a plant hormone in these algae, that auxin signaling occurs and that it plays similar roles in development as in land plants (Lau et al., 2009; De Smet et al., 2011; Zhang and van Duijn, 2014).

To gain a better understanding of the role of auxin and auxin transport in *Chara* cells, we aimed to investigate the well-known membrane potential and ion transport responses of higher plant cells to stimulation with exogenous auxin in *Chara* internodal cells.

Materials and Method

Algae

Chara corallina was cultured indoors at room temperature in aquaria filled with artificial pond water (APW) containing 0.1mM KCl, 0.1mM $CaCl_2$ and 0.1mM NaCl (pH about 6.0), and forest soil as described earlier (Berecki et al., 1999) under 8/16 light/dark conditions. Nutrients from the forest soil diffuse into the water to support growth of the algae. For the experiments fully grown algae were selected for their internodal cells to be used in measurements.

Membrane potential measurements

Changes of membrane potential were measured using the K-anesthesia method (Shimmen et al., 1976). Single internodal cells with node cells on both ends were separated from the plants and put in a chamber with two pools isolated by Vaseline with the volume of 3- 4ml each (Fig. 1). One pool (A) was filled with APW, the other one (B) was filled with 55 mM KCl dissolved in APW (unless stated otherwise). Electrical potential differences were measured by insertion of Ag/AgCl electrodes in the pools connected to an amplifier Model 750 (W.P. Instruments) in current clamp mode. Results were recorded and analyzed using the software package Clampex7 (Axon Instruments). The measurements took place inside a closed Faraday cage on a vibration free table to avoid disturbances from the environment, and to suppress the band formation ability of *Chara* cells, which may cause unexpected influences on the measurement, there was no extra light supplemented inside the shaded unit.

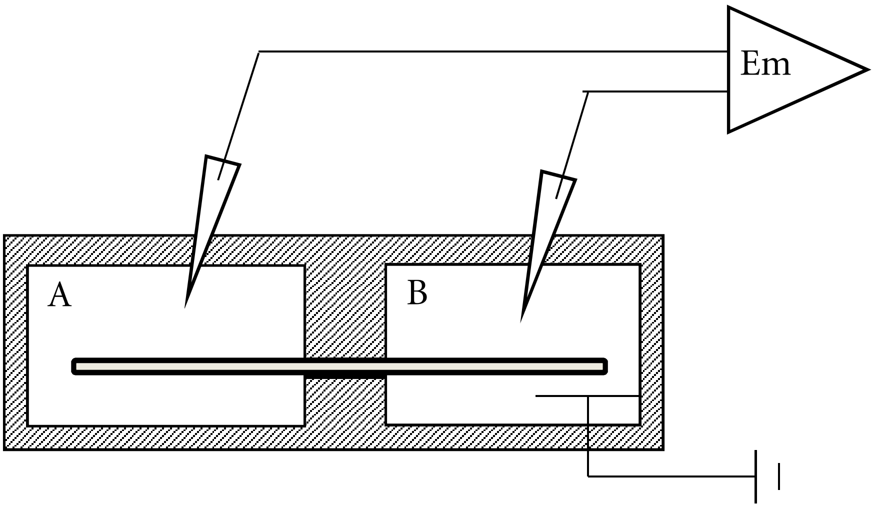

Figure 1. Membrane potential measurement set-up according to Shimmen et al. (1976). Single internodal cells with node cells on both ends were separated from the plants and put in a chamber with two pools isolated by vaseline. Pool A was filled with APW, pool B was filled with 55 mM KCl dissolved in APW (unless stated otherwise). Electrical potential difference between the two pools is measured by insertion of an Ag/AgCl electrode in each pool connected to a current clamp amplifier.

The effect of pH differences was tested with two or three levels for different concentrations of K^+ in the solution (0.1 mM, 1 mM, 10 mM and 55 mM).

Influence of three different types of auxin (IAA, 1-NAA, 2-NAA) on the cell membrane potential was tested for different concentrations (10^{-8}M, 10^{-7}M, 10^{-6}M, 10^{-5} M). IAA and the other two homologs were dissolved with ethanol at the concentration of 10^{-2}M and stored. Before use the stock was diluted with APW to final concentrations of 10^{-8}M to 10^{-5}M. To ensure that addition of auxin did not alter the pH, the pH of auxin solution was adjusted to the original APW pH. The addition of auxin was done carefully along the cell at the opposite side of the electrodes to avoid high peak concentration of auxin near the cells due to lack of dilution, as well as to avoid mechanical stimulation of the cell (Shimmen, 1997).

Ion flux measurements

Net fluxes of H^+ and K^+ were measured noninvasively using scanning ion-selective electrode technique. We used the ASET system (Automated Scanning Electrode Technique) from Science Wares Inc. The principle of this method and instrument are detailed in Jones et al. (1995), Shabala et al. (1997) and, Li et al. (2010).

Probes were fabricated from tributylchlorosilane (Fluka 90796) silanized 1.5 mm x 1.17 mm thin wall capillaries (Harvard Apparatus) pulled on a Sutter P-1000 pipette puller to give a 10 µm tip opening. Probes were backfilled with either 100 mM KCl for K^+-measurements or 15 mM NaCl, 40 mM KH_2PO_4, pH 7,0 (with NaOH) for pH measurements. The tip was filled with 150-300 µm K^+ LIX (Fluka 60031) or H^+ LIX (Fluka 95297) respectively through brief submersion of the tip in LIX held in a capillary.

In all the measurements below, the position of the probe tips was alternated with a 20 µm step between 50-70 µm from the cell surface in a perpendicular direction. At each location, the ion concentration was measured for 10 s allowing the solution to settle after the motion of the probes. The concentration difference between the two locations was directly calculated and reported as the flux. The data was recorded by ASET and further analyzed using Excel (Microsoft Corporation).

The influences of IAA, fusicoccin (FC), pH and light on the net fluxes of H^+ and K^+ were tested.

Banding formation

Band formation solution (BFS) was used to detect the acid/alkaline bands of *Chara.* BFS was freshly prepared by adding 0.5 mM $NaHCO_3$ and 5 mg/100 ml phenol red to APW (color range of phenol red: yellow while pH below 6.8, red while pH above 8.2). pH was adjusted to around 6.5 for a lighter background.

Results and discussion

Membrane potential measurements

In higher plants membrane potential hyperpolarization is a well-established rapid response to application of auxin. In order to study the auxin responsiveness of *Chara* intermodal cells, the effect of auxin on the membrane potential was studied. The membrane potential was measured with the 'K-anesthesia' method (Shimmen et al., 1976). First, some basic responses of the membrane potential were measured, such as pH dependence and K^+ dependence, followed by applications of auxin.

pH and K+ dependence

The membrane potential of *Chara* cells has been shown to be both dependent on the intracellular and extracellular potassium concentration ratio and the ATP (and pH) dependent activity of proton transport (Shimmen et al., 1994; Tazawa and Shimmen, 2001). To test the membrane potential measurements and to be able to discriminate between auxin-induced membrane potential changes and pH-induced membrane potential changes we first studied the effect of APW with different pH values and K^+ concentrations on the membrane potential as measured with the 'K-anesthesia' method.

In the experiment the membrane potential was measured for varying K^+ concentrations in pool B while in pool A standard APW (with 0.1 mM K^+) was used. Figure 2 shows the relationship between the measured membrane potential with this method and the ^{10}Log of the ratio of the K^+ concentration in the two pools. The membrane potential shows to be strongly potassium dependent and follows a linear relationship with the ^{10}Log of the potassium concentration ratio between the pools. Similar strong potassium dependency was found in earlier studies (Shimmen and Tazawa, 1977; Shimmen, 2001).

With regard to the sensitivity of the membrane potential to the extracellular pH it has been shown that this effect can be much stronger if the cells are in full light as compared to more dark conditions (Saito and Senda, 1973; Felle and Bentrup, 1976) which mainly is due to the presence of MgATP that provides the energy for the H^+-ATPase activity (Kaeamura et al., 1980). In the absence of ATP the membrane potential dependence on the extracellular pH is rather weak and completely absent if no MgATP is present.

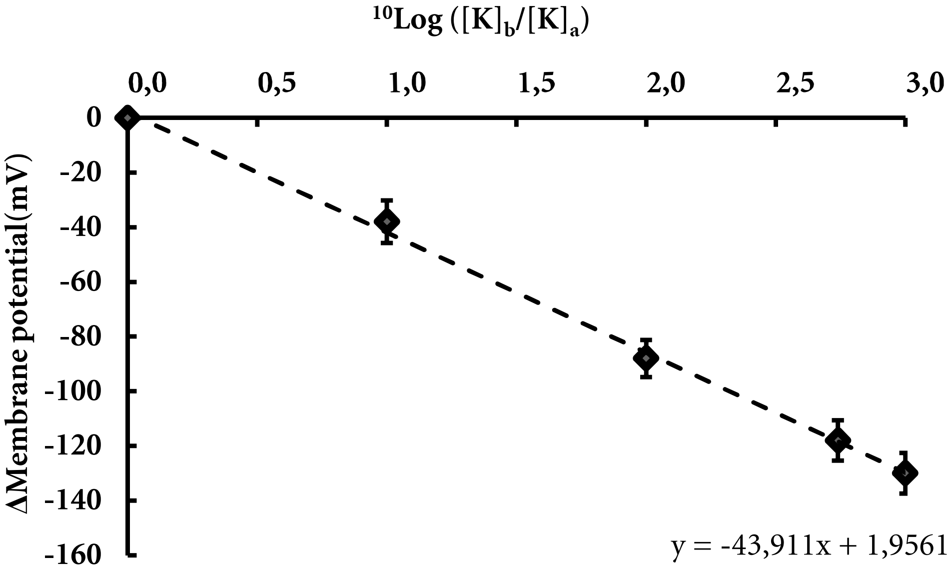

Figure 2. Membrane potential as measured for different potassium concentrations in pool B at a constant potassium concentration in pool A. Measured values represent the average of 6 independent measurements on different cells. Error bars are the standard error. The dashed line is a linear fit through the data points.

In our experiments the membrane potential was not strongly dependent on the extracellular pH, which may be attributed the rather low light conditions in the experimental set up. Maximal membrane potential changes were recorded for conditions with APW in both pools with an extracellular pH of about 5.2 in pool A and 7.3 in pool B of about –13.8 ± 4.1 mV (n=4). With increasing potassium concentration in pool B the effect of different pHs' in pool B on the membrane potential became much smaller. At 55 mM KCl in pool B with pH switching from 5.2 to 7.3 (pool A with standard APW at pH 5.2) the membrane potential change amounted only about 2.5 mV (n=2).

From our measurements we conclude that the membrane potential is both pH and K^+ concentration dependent. The concentration of K^+ in the bath solution has a significant influence on the membrane potential. For Increasing pH values we find more negative membrane potentials, but the changes caused by pH are mitigated in the presence of high concentrations of K^+. These findings are in agreement with earlier membrane potential measurements on *Chara* cells (Shimmen et al., 1994; Shimmen and Wakabayashi, 2008) and look similar to effects of pH and potassium on the membrane potential of higher plant cells (Lew, 1991; Katicheva et al., 2014).

Auxin dependence

Different concentrations of IAA, 1-NAA and 2-NAA in APW (pH 6.0) were added to pool A and the effects on the membrane potential were recorded and analyzed. From an IAA concentration of about 10^{-6} M and higher a change in membrane potential could be recorded (Fig. 3). After addition of IAA at sufficient concentration the potential changes rapidly (within a few seconds). The auxin analogues 1-NAA, 2-NAA were much less effective in inducing a membrane potential change. At a concentration of 1.25×10^{-5} M the average membrane potential change with 1-NAA was -2.7 ± 1.0 mV (n=6), and was for 2-NAA -7.7 ± 1.1 mV (n=6). This is much less than was recorded for IAA, which amounted -15.7 ± 1.2 mV (n=6) at the same concentration.

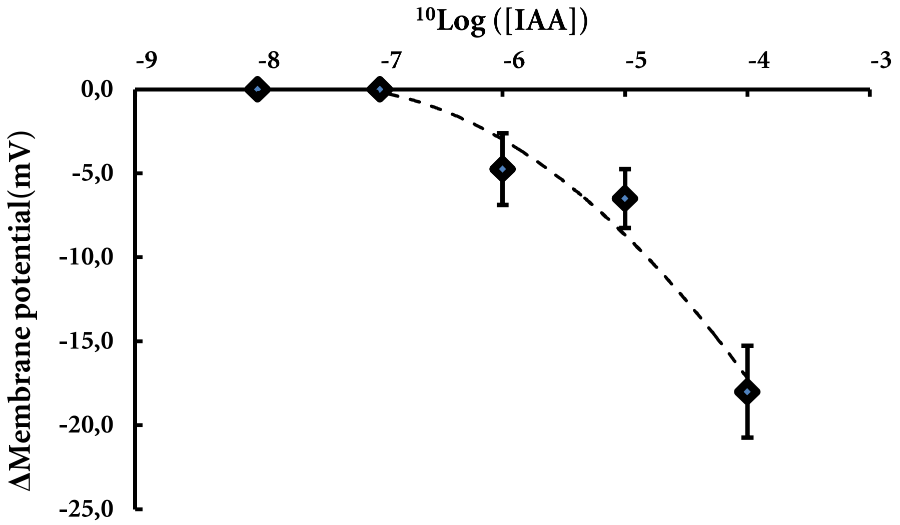

Figure 3. Membrane potential changes caused by different concentrations of IAA. Measured values represent the average of 5 independent measurements on different cells. Error bars are the standard error. The dashed line shows the trend.

Although all three tested auxins can induce a (small) membrane potential change, the effect of IAA is more obvious. The IAA concentration necessary to induce a significant membrane potential change can be regarded as comparable to auxin concentrations that are effective in higher plants with respect to induction of gene expression and differentiation (Tatematsu et al., 2004; Sun et al., 2013; Baster et al., 2013; Lee et al., 2009) as well as to auxin-induced membrane potential changes in higher plant cells which are typically reported to be effective in the range of 1 - 100 µM auxin (Van Duijn and Heimovaara-Dijkstra, 1994; Felle et al., 1991; Kirpichnikova et al., 2014; Ephritikine et al., 1987; Barbier- Brygoo et al., 1989). The auxin-induced membrane potential changes in higher plant cells typically are in the order of -5 to -20 mV. These values and concentrations are well in agreement with the results we find in *Chara* intermodal cells.

Ion flux measurements

Auxin-induced membrane potential changes may be accompanied by different ion fluxes. Typically, proton and potassium fluxes are reported upon application of auxin to higher plant cells. As in land plants auxin is shown to be able to activate proton pumps directly as well as activate the synthesis of proton pump proteins (Hager et al., 1991; Hager, 2003; Takahashi et al., 2012), H^+ -fluxes may be expected upon auxin application to *Chara* cells. The proton pump also is a determinant in the membrane potential of *Chara* cells (see above and Tsutsui et al., 2001; Beilby, 2015). In addition, potassium fluxes are also reported upon auxin application to higher plant cells (Blatt et al., 1994; Claussen et al., 1996; Hager, 2003; Fuchs et al., 2006) and potassium is also an indispensable player in the resting membrane potential in *Chara* (see results above and Shimmen et al. ,1994).

In these experiments we chose H^+ and K^+ as our main target ions. The vibrating probe technique was used to measure real-time ion fluxes through *Chara* membranes.

Salt and light dependence

The responsiveness of the electrodes and the cells were tested by application of salt stress to the cells. Upon application of a salt shock the sensitivity of the H^+ and K^+ probes and the reactivity of the cells could be established. Two different NaCl concentrations were applied to the cells. In repetition 1 ml 100 mM NaCl-APW was added into 4 ml bath solution resulting in a final concentration of 25 mM NaCl followed by 2 ml 400mM NaCl-APW resulting in a concentration of 200 mM NaCl. This resulted with the low NaCl concentration (25 mM) stimulation in an immediate efflux of K^+ of a magnitude of about 50 $nmol \cdot m^{-2} \cdot s^{-1}$, and a slight change in the H^+ flux of about 4 $nmol \cdot m^{-2} \cdot s^{-1}$. When the high level (200 mM) NaCl stimulation was applied, there was an immediate activation of K^+ transport with a further activation of the proton flux (with a magnitude of 10-20 $nmol \cdot m^{-2} \cdot s^{-1}$), followed by several long lasting extreme peaks of K^+ efflux up to 600-700 $nmol \cdot m^{-2} \cdot s^{-1}$. An example of the responses in such an experiment is shown in figure 4. From the responses on the addition of NaCl we conclude that both the cells and measurement system are functional for the measurement of K^+ and H^+ fluxes.

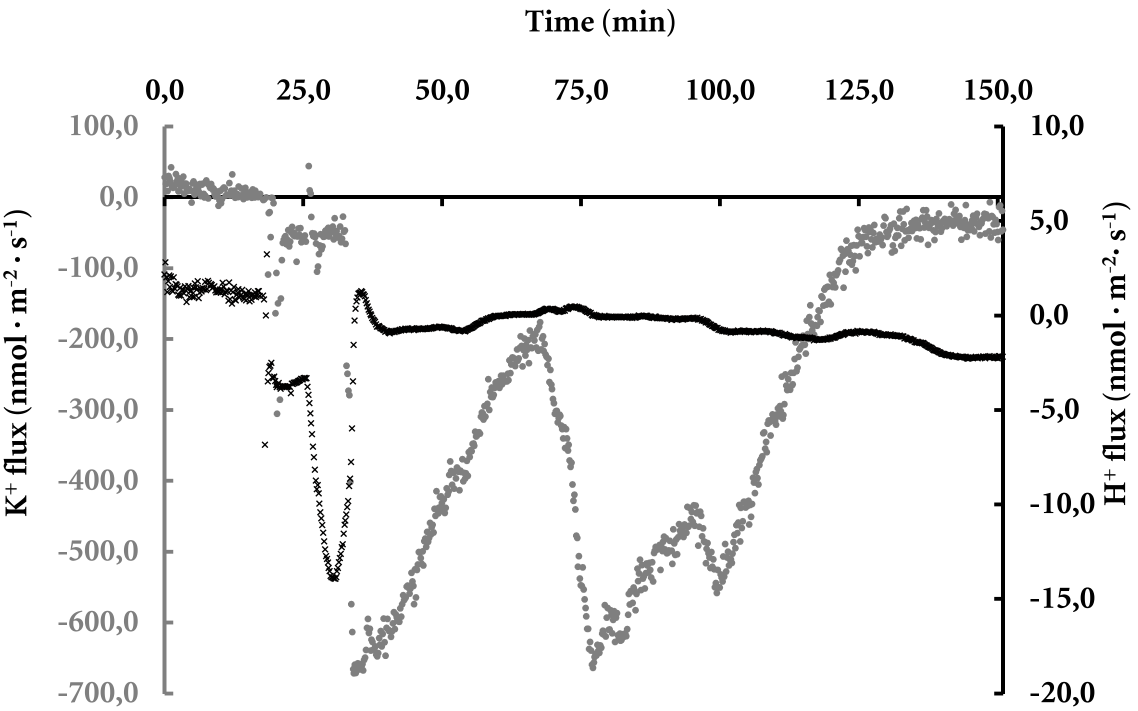

Figure 4. An example of salt stimulation. 200 mM NaCl stimulation was introduced at 20 min time point and the response was recorded for the next two hours. Gray dots indicate the real time recording of K^+ flux, black crosses indicate the real time recording of H^+ flux.

For measuring the H^+ and K^+ flux responses to auxin the occurrence of pH band formation in *Chara* intermodal cells (Fisahn et al., 1989) may complicate the analysis, as the responses may be different in the different pH zones along the cell. Therefore, in first instance we used the vibrating probe system to identify the pH banding and the accompanying fluxes along the *Chara* internodal cells.

In the formation of the pH banding of healthy *Chara* cells under light stimulation, the proton pumps are proposed to be the driving force (Schmolzer et al., 2011). During the experiments, we observed that around 80-90% of the surface area of *Chara* cells is indicated by phenol red to be acid (Fig. 5, insert). In our system the H^+ and K^+ selective probes were moved along the longitudinal axis of the *Chara* internodal cells over a certain distance to cover at least one acid band and one adjacent alkaline band. This resulted in H^+ and K^+ flux data for the different positions along the cell that could be linked to the acid and alkaline regions. The average fluxes from a representative cell in the stable state are shown in figure 5. Movement of the tip of the vibrating probe along the cell length showed clear proton influx and efflux zones (Fig. 5), indicating the acid (proton efflux) and alkaline (proton influx) zones. Among these different zones, the probes also passed three chloroplast-free neutral line points (see Foissner et al., 2015 and P2, P7, P9 in figure 5). No evidence showed any link between the neutral line and the pH banding pattern, which matches the observation of former research (Foissner et al., 2015). The K^+ probes showed that the flux of K^+ was mainly present as a K^+ influx. Though there was no clear influx efflux pattern for K^+, a correlation between the H^+ and K^+ fluxes is present. K^+ influx was mainly present in the alkaline band (proton influx zone) and usually showed large variations in amplitude. Hence, the relatively large standard deviations of K^+ influx in the alkaline zones (Fig. 5). While in the acid band, K^+ uptake activity is much less, and only relatively small K^+ influxes were measured. In contrast to this with mechanical or chemical stimulations, K^+ efflux could also be recorded in the acid zone together with an enlarged H^+ efflux, as see in figure 4.

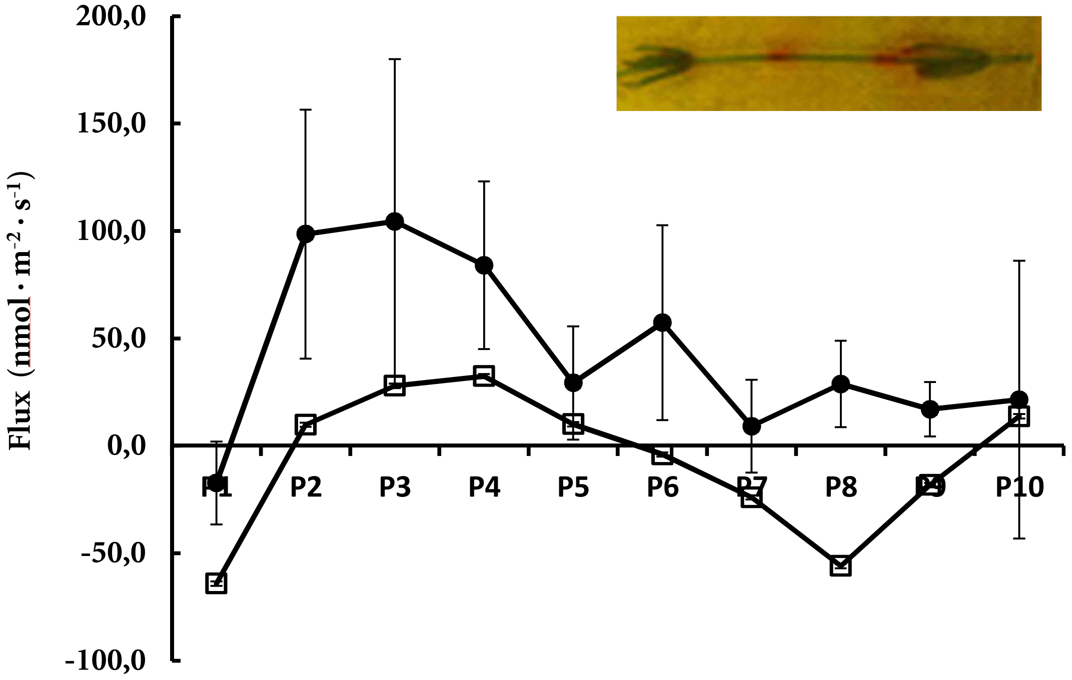

Figure 5. H^+ and K^+ fluxes for 10 different positions (P1-P10) along the longitudinal axis of the cell. Distance between each measuring point ranges between 1- 5mm. Every data point is an average of 5-10 min measurements of real-time flux with standard deviation. P2, P7, P9 are measurements done beside three continuously neutral lines points along the probe moving direction. P10 was measured near the cell node of the same moving direction. Positive flux in the figure represents an influx of positive ions. Solid circle indicates the K^+ flux. Open squares indicate the H^+ flux.

Light, known to be the trigger of the band formation, as another activator of proton pumps, was tested by switching on or off the microscope light. As expected, light can trigger an increase of the efflux or influx of protons dependent on the position along the axis of *Chara* cells. At the boundary of different bands, the proton flux showed fluctuations (unstable patterns) between influx and efflux during the test period (0.5-1 hour). Together with the proton flux, the flux of potassium also showed a strong response to the light, with more active influx in the alkaline band upon light stimulation. Switching off the light caused an immediate reduction of potassium influx or even triggered an efflux. An example is given in figure 6.

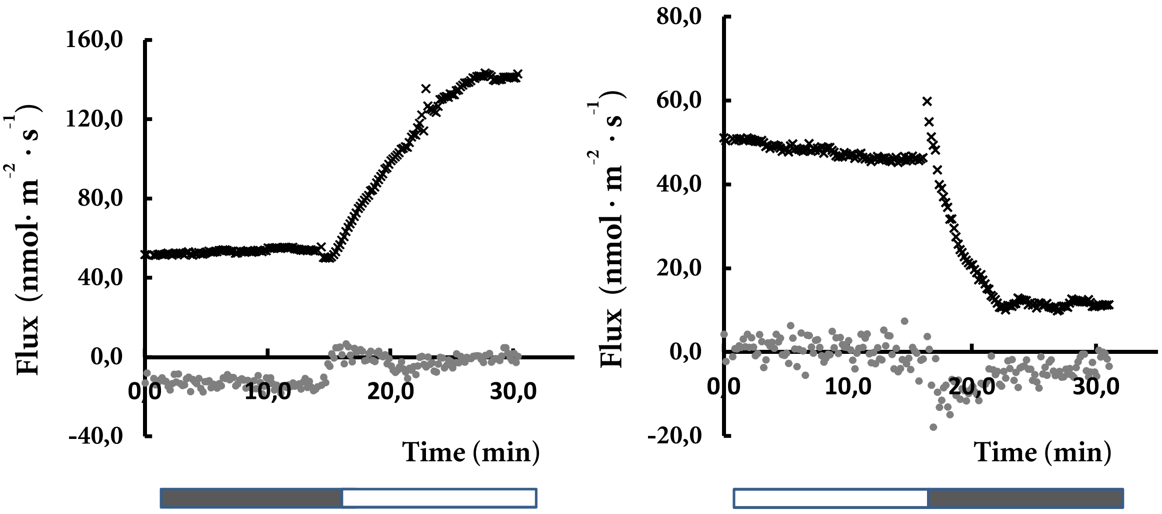

Figure 6. An example of light stimulation of the real-time H^+, K^+ fluxes. Gray dots indicate the real time recording of K^+ flux, black crosses indicate the real time recording of H^+ flux. Bars below indicates the light conditions. White bar shows the period with light on and dark bar shows the period with light off.

Auxin dependence

The effect of IAA on H^+ and K^+ fluxes was tested with the vibrating probe system. Since IAA is an organic weak acid a disturbance of the solution pH would be calculated as proton flux based on the principle of the measurement technique. Figure 7 shows an example of pH influence on the fluxes in the acid band. Upon the addition of 1 ml APW with pH 4.0 to 3 ml APW with pH 5.1 a peak H^+ flux is induced, while there are no related K^+-flux responses.

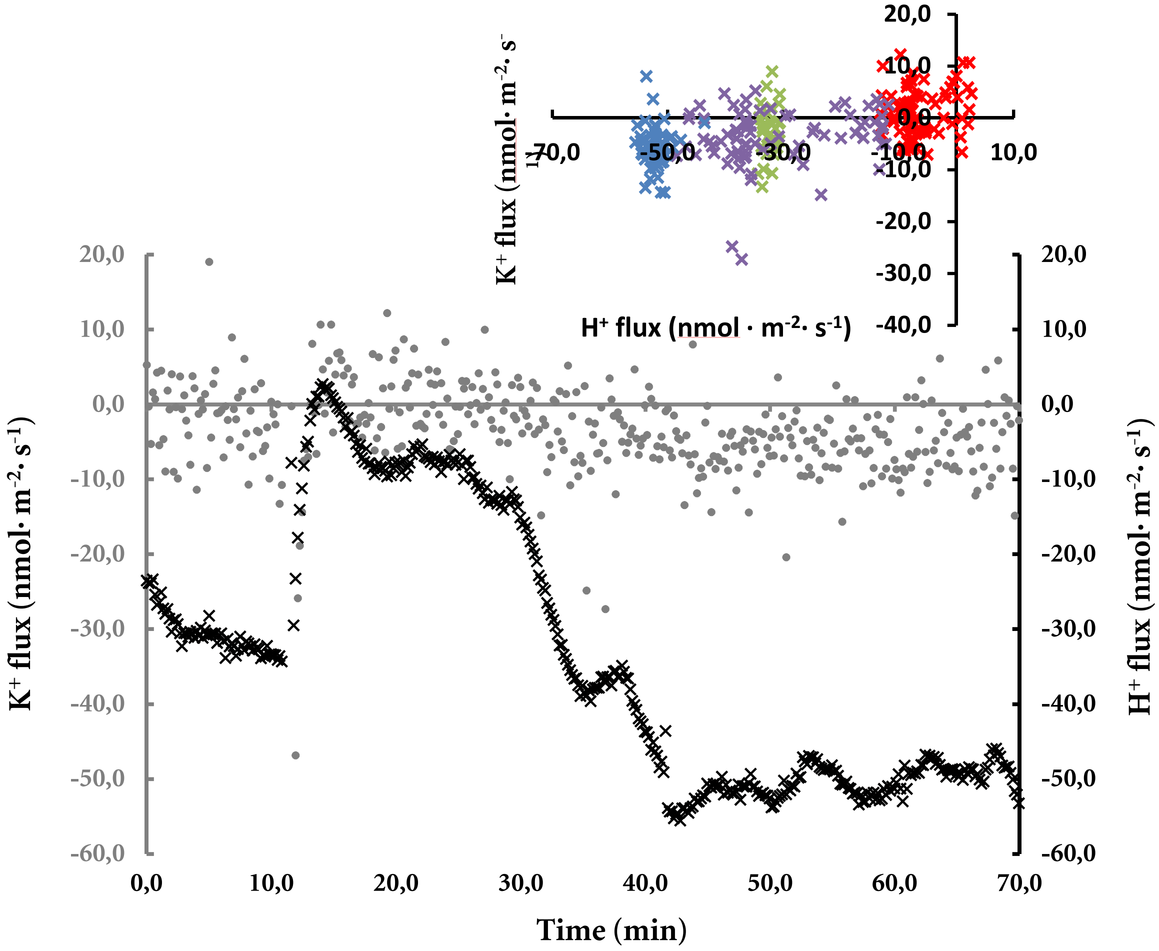

Figure 7. An example of pH stimulation. 1 ml pH 4.0 APW was added into bath solution (pH 5.0 APW) at 10 min. The response was recorded for the next hour. Gray dots indicate the real time recording of K^+ flux, black crosses indicate the real time recording of H^+ flux. The insert shows the relationship between H^+ and K^+ during a certain period. Green crosses represent the original stable state of the H^+, K^+ fluxes. Red crosses represent the first 15 min after the stimulation. Purple crosses represent the next 15 min and blue crosses represent the final stable state after the stimulation.

To separate the possible IAA influence on the PM proton pump from the acidification of the solution caused by the addition of IAA, the original bath pH without IAA was adjusted to the pH of the IAA solution (around pH 4.0) for the measurements of IAA-induced fluxes. In this situation no clear pH banding could be detected along the cell. H^+ and K^+ fluxes were measured continuously during slowly and evenly adding 1 ml 4×10^{-5}M IAA to 3 ml APW (final concentration of 10^{-5} M IAA). This addition showed no strong changes in H^+ flux (the small pH shifts are hard to avoid due to the unstable pH of the IAA solution). However, clear IAA-induced K^+ fluxes (in the range of about 100 $nmol{\cdot}m^{-2}{\cdot}s^{-1}$) were seen in most of cases (5 out of 6). A typical example is shown in figure 8.

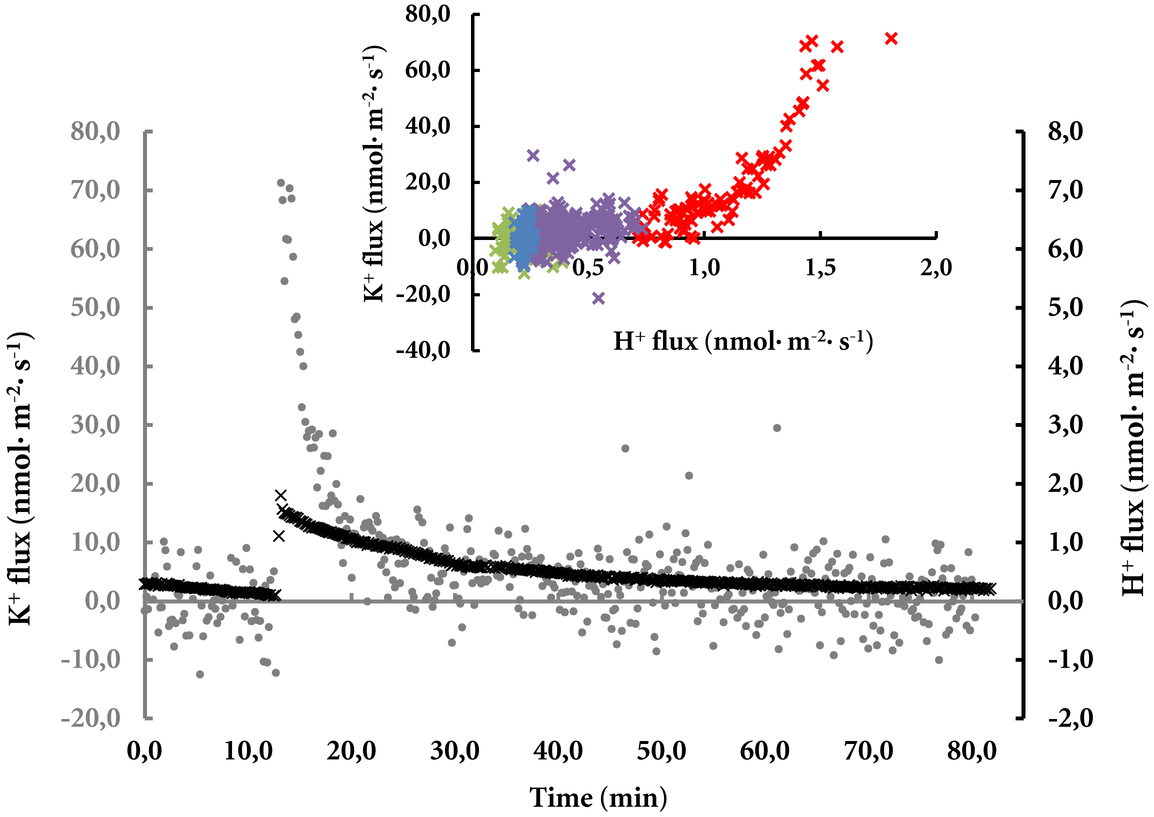

Figure 8. An example of the effect of IAA on ion-fluxes. IAA was introduced into the bath solution at 10 min. The response was recorded for the next hour. Gray dots indicate the real time recording of K^+ flux, black crosses indicate the real time recording of H^+ flux. The insert shows the relationship between H^+ and K^+ during a certain period. Green crosses represent the original stable state of the H^+, K^+ fluxes. Red crosses represent the first 15 min after the stimulation. Purple crosses represent the next 15 min and blue crosses represent the final stable state after the stimulation.

In *Chara* cells, PM H^+-ATPases are believed to be the driving force of the pH banding phenomenon and the main donator to the H^+ flux through the membrane. PM H^+-ATPases are well known to exist in fungi and higher plants and the regulation mechanisms has also been widely studied in yeast and many land plant species (Morsomme and Boutry, 2000). The C-terminus auto-inhibition domain functions as a main switch in activating the pump function. In yeast, the proton pump is activated by stepwise phosphorylation of two tandemly positioned residues, Ser-911 and Thr-912, at the C-terminus (Lecchi et al., 2007) while in land plants, a conserved penultimate threonine (pT-H^+-

ATPases) at the C-terminus is playing a key role in the regulation through phosphorylation (Wielandt et al., 2015). Based on the acid-growth theory, auxin has been proved of inducing the phosphorylation of penultimate threonine to create a binding domain with 14-3-3 proteins and further activating the PM H^+-ATPases in Arabidopsis (Takahashi et al., 2011). Nevertheless, in algea and lower plants the structure of the PM H^+-ATPases are still unknown. In moss the co-existence of a non-pT type PM H^+-ATPases has been confirmed (Okumura et al., 2012a) and there is so far no evidence of the pT-H^+-ATPase in algea species (with/without sequence information) including *Chara*.

The fungal toxic fusiccocin (FC), due to its ability to enhance the binding of 14-3-3 to the phosphorylated C-terminal domain of the PM H^+-ATPases in land plants, has been widely used in the research related to PM H^+-ATPases activities (Jahn et al., 1996). Effects of FC on the photosystem II (PSII) effective quantum yield and extracellular pH in the light-induced pH banding in *Chara* has been reported (Bulychev et al., 2005). However, as no proton fluxes were induced by IAA in the Chara internodes it may be expected that FC is also not effective. Indeed, the addition of different concentrations of FC did not resultin a change ofthe measured H^+ fluxes along the *Chara* internode cells (data not show). The apparent discrepancy between the reported FC-induced increased acidification in the banding pattern (Bulychev et al., 2005) and our results may be due to timing in experimentation (Bulychev et al., 2005 reported on an effect more than 1 h after FC application) and the age of the plant material (fully grown in our experiments) may play a role as well. Our results are definitely not enough to rule out the involvement of phosphorylation and 14-3-3 protein in the regulation of *Chara* PM H^+-ATPases. Yet the available sequence data indicates quite a variety in the PM H^+-ATPases C-terminus among different species of algea (Okumura et al., 2012b). This variety would also embrace the possibility of other new regulation mechanisms.

Conclusions

Based on the above data, it seems that the plant hormone auxin does induce cellular physiological responses in *Chara* cells, such as membrane potential changes and K^+ fluxes, that are also seen in higher plants.

On the other hand, the well documented (Rober-Kleber et al. 2003; Takahashi et al., 2012) induction of H^+-ATPase activity by auxin in higher plants was not found in the *Chara* cells we used. The age and developmental stage of the cells may be a relevant factor in this. Young, developing cells may show the induction of proton fluxes by IAA. Future research on the relationship between IAA and *Chara* development is necessary to resolve this possibility

Though *Chara* cells have been used as an interesting research target for almost half a century, the lack of gene sequences information has slowed down the understanding progress. Further research would be interesting and necessary to find out the characteristics of these possible new type of proton pumps and further understand the auxin regulation mechanism in these plant-like algea systems.

Acknowledgements

We thank Marco Vennik (Fytagoras) for technical support in membrane potential measurements and Kees J.M. Boot (Leiden University) for the proof reading and suggestions. S. Zhang was financially supported by Chinese Scholarship Council (2011635073) and Stichting (Foundation) Single Cell Research (SCSR06-01-15).

References

Adamowski, M. and Friml, J. (2015). PIN-dependent auxin transport: action, regulation, and evolution. *The Plant Cell,* 27: 20-32.

Barbier-Brygoo, H., Ephritikhine, G., Klambt, D., Ghislain, M., Guern, J. (1989). Functional evidence for an auxin receptor at the plasmalemma of tobacco mesophyll protoplasts. *PNAS,* 86: 891-5.

Baster, P., Robert, S., Kleine-Vehn, J., Vanneste, S., Kania, U., Grunewald, W., De Rybel, B., Beeckman, T., Friml, J. (2013). SCF $^{TIR1/AFB}$-auxin signalling regulates PIN vacuolar trafficking and auxin fluxes during root gravitropism. *The EMBO J.*, 32: 260-74.

Beilby, M.J. (2015). Salt tolerance at single cell level in giant-celled Characeae. *Front Plant Sci.*, 6: 226. doi: 10.3389/fpls.2015.00226.

Berecki, G., Varga, Z., Van Iren, F., Van Duijn, B. (1999). Anion channels in *Chara corallina* tonoplast membrane: calcium dependence and rectification. *J. Membr. Biol.*, 172: 159–168.

Berleth, T., Krogan, N.T., Scarpella, E. (2004). Auxin signals - turning genes on and turning cells around. *Curr. Opin. Plant Biol.*, 7: 553-63.

Blatt, M.R. and Thiel, G. (1994). K^+ channels of stomatal guard cells: bimodal control of the K^+ inward-rectifier evoked by auxin. *The Plant J.*, 5 (1): 55-68.

Boot, K.J.M., Libbenga, K.R., Hille, S.C., Offringa, R., Van Duijn, B. (2012). Polar auxin transport: an early invention. *J. Exp. Bot.*, 63 (11): 4213-18. doi: 10.1093.jxb.ers106.

Bulychev, A.A., Van den Wijngaard, P.W.J., De Boer, A.H. (2005). Spatial coordination of chloroplast and plasma membrane activities in *Chara* cells and its disruption through inactivation of 14-3-3 proteins. *Biochemistry (Mosc.)*, 70 (1): 55–61.

Christian, M., Steffens, B., Schenck, D., Burmester, S., Bottger, M., Luthen, H. (2006). How does auxin enhance cell elongation? Roles of auxin-binding proteins and potassium channels in growth control. *Plant Biol.*, 8: 346-52.

Claussen, M., Luthen, H., Blatt, M., Bottger, M. (1996). Axuin-induced growth and its linkage to potassium channels. *Planta*, 201: 227-34.

Cooke, T.J., Poli, D.B., Sztein, A.E., Cohen, J.D. (2002). Evolutionary patterns in auxin action. *Plant Mol. Biol.*, 49: 319-38.

De Smet, I., Voß, U., Lau, S., Wilson, M., Shao, N., Timme, R.E., Swarup, R., Kerr, I., Hodgman, C., Bock, R., Bennett, M., Jurgens, G., Beeckman, T. (2011). Unraveling the evolution of auxin signaling. *Plant Physiol.*, 155: 209-21.

Di, D., Zhang, C., Guo, G. (2015). Involvement of secondary messengers and small organic molecules in auxin perception and signalling. *Plant Cell Rep.*, 34: 895-904.

Dibb-Fuller, J.E. and Morris, D.A. (1992). Studies on the evolution of auxin carriers and phytotropin receptors: Transmembrane auxin transport in unicellular and multicellular Chlorophyta. *Planta*, 186: 219-26.

Enders, T.A. and Strader, L.C. (2015). Auxin activity: past, present, and future. *Am. J. Bot.*, 102 (2): 180-96.

Ephritikhine, G., Barbier-Brygoo, H., Muller, J.F., Guern, J. (1987). Auxin effect on the transmembrane potential difference of wild-type and mutant tobacco protoplasts exhibiting a differential sensitivity to auxin. *Plant physiol.*, 83: 801-4.

Felle, H. and Bentrup, F.W. (1976). Effect of light upon membrane potential, conductance and ion fluxes in *Riccia fluitans. J. Membr. Biol.*, 27: 153-70.

Felle, H., Peters, W., Palme, K. (1991). The electrical response of maize to auxins. *Biochim. Biophys. Acta*, 1064: 199-204.

Feraru, E., Vosolsobe, S., Feraru, M.I., Petrášek, J., Kleine-Vehn, J. (2012). Evolution and structural diversification of PILS putative auxin carriers in plants. *Front Plant Sci.*, 3: 1-13.

Fisahn, J., McConnaughey, T., Lucas, W.J. (1989). Oscillations in extracellular current, external pH and membrane potential and conductance in the alkaline bands of *Nitella* and *Chara. J. Exp. Bot.*, 40 (220): 1185-93.

Foissner, I., Sommer, A., Hoeftberger, M. (2015). Photosynthesis-dependent formation of convoluted plasma membrane domains in *Chara* internodal cells is independent of chloroplast position. *Protoplasma*, 252: 1085-96.

Fuchs, I., Philippar, K., Hedrich, R. (2006). Ion channels meet auxin action. *Plant Biol.*, 8: 353-9.

Fujita, T. and Hasebe, M. (2009). Convergences and divergences in polar auxin transport and shoot development in land plant evolution. *Plant Signal Behav.*, 4: 313-5.

Hager, A. (2003). Role of the plasma membrane H^+-ATPase in auxin-induced elongation growth: historical and new aspects. *J. Plant Res.*, 116: 483-505.

Hager, A., Debus, G., Edel, H.G., Stransky, H., Serrano, R. (1991). Auxin induces exocytosis and the rapid synthesis of a high-turnover pool of plasma-membrane H^+-ATPase. *Planta*, 185: 527-37.

Jahn, T., Johansson, F., Luthen, H., Volkmann, D., Larsson, C. (1996). Reinvestigation of auxin and fusicoccin stimulation of the plasma-membrane H^+-ATPase activity. *Planta*, 199: 359-65.

Jones, D.L., Shaff, J.E., Kochian, L.V. (1995). Role of calcium and other ions in directing root hair tip growth in Limnobium stoloniferum. *Planta,* 197: 672–680.

Katicheva, L., Sukhov, V., Akinchits, E., Vodeneev, V. (2014). Ionic nature of burn-induced variation potential in wheat leaves. *Plant Cell Physiol.*, 55 (8): 1511-9.

Kawamura, G., Shimmen, T., Tazawa, M. (1980). Dependence of the membrane potential of *Chara* cells on external pH in the presence or absence of internal adenosinetriphosphate. *Planta*, 149: 213-8.

Kirpichnikova, A.A., Rudashevskaya, E.L., Yemelyanov, V.V., Shishova, M.F. (2014). Ca^{2+}-Transport through plasma membrane as a test of auxin sensitivity. *Plants*, 3: 209-22.

Kramer, E.M., Ackelsberg, E.M. (2015). Auxin metabolism rates and implications for plant development. *Front. Plant Sci.*, 6: 150. doi: 10.3389/fpls.2015.00150

Lau, S., Shao, N., Bock, R., Jürgens, G., De Smet, I. (2009). Auxin signaling in algal lineages: fact or myth? *Trends Plant Sci.*, 14: 182-8.

Lee, D.J., Park, J.W., Lee, H.W., Kim, J. (2009). Genome-wide analysis of the auxin-responsive transcriptome downstream of iaa1 and its expression analysis reveal the diversity and complexity of auxin-regulated gene expression. *J. Exp. Bot.*, 60 (13): 3935-57.

Lew, R.R. (1991). Electrogenic transport properties of growing Arabidopsis root hairs: the plasma membrane proton pump and potassium channels. *Plant Physiol.*, 97 (4): 1527-34.

Morris, D.A. (2000). Transmembrane auxin carrier systems-Dynamic regulators of polar auxin transport. *Plant Growth Regul.*, 32: 161-72.

Okumura, M., Takahashi, K., Inoue, S., Kinoshita, T. (2012). Evolutionary appearance of the plasma membrane H^+-ATPase containing a penultimate threonine in the bryophyte. *Plant Signal Behav.,* 7 (8): 979-82.

Okumura, M., Inoue, S., Takahashi, K., Ishizaki, K., Kohchi, T., Kinoshita, T. (2012). Characterization of the plasma membrane H^+-ATPase in the liverwort *Marchantia polymorpha. Plant Physiol.*, 159: 826-34.

Osakabe, Y., Arinaga, N., Umezawa, T., Katsura, S., Nagamachi, K., Tanaka, H., Ohiraki, H., Ymada,K., Seo, S.U., Abo, M., Yoshimura, E., Shinozaki, K., Yamaquchi-Shinozaki, K. (2013). Osmotic stress responses and plant growth controlled by potassium transporters in Arabidopsis. *The Plant Cell*, 25: 609-24.

Philippar, K., Ivashikina, N., Ache, P., Christian, M., Lüthen, H., Palme, K., Hedrich, R. (2004). Auxin activates KAT1 and KAT2, two K^+-channel genes expressed in seedlings of *Arabidopsis thaliana. Plant J.*, 37 (6): 815-27.

Qin, Y. and Dong, J. (2015). Focusing on the focus: what else beyond the master switches for polar cell growth. *Mol. Plant*, 8: 582-94.

Qiu, Y.L. and Palmer, J.D. (1992). Phylogeny of early land plants: insight from genes and genomes. *Trends Plant Sci.*, 4: 26-30.

Rober-Kleber, N., Albrechtova, J.T.P., Fleig, S., Huck, N., Michalke, W., Wagner, E. Speth, V., Neuhaus, G., Fischer-Iglesias, C. (2003). Plasma membrane H^+-ATPase is involved in auxin-mediated cell elongation during wheat embryo development. *Plant physiol.*, 131 (3): 1302-12.

Saito, K. and Senda, M. (1973). The effect of external pH on the membrane potential of *Nitella* and its linkage to metabolism. *Plant Cell Physiol.*, 14: 1045-52.

Schmolzer, P.M., Hoftberger, M., Foissner, I. (2011). Plasma membrane domains participate in pH banding of *Chara* internodal cells. *Plant Cell Physiol.*, 52 (8): 1274-88.

Shabala, S.N., Newman, I.A., Morris, J. (1997). Oscillations in H^+ and Ca^{2+} ion fluxes around the elongation region of corn roots and effects of external pH. *Plant Physiol.*, 133: 111-118.

Shimmen, T. (1997). Studies on mechano-perception in Characeae: decrease in electrical membrane resistance in receptor potentials. *Plant Cell Physiol.*, 38 (11): 1298-301.

Shimmen, T. (2001). Studies on electrogenesis under high K^+ concentrations in internodal cells of *Chara coralline. J. Plant Res.*, 114: 59-66.

Shimmen, T. and Tazawa, M. (1977). Control of membrane potential and excitability of *Chara* cells with ATP and Mg^{2+}. *J. Membr. Biol.*, 37: 167-92.

Shimmen, T. and Wakabayashi, A. (2008). Involvement of membrane potential in alkaline band formation by intermodal cells of *Chara coralline. Plant Cell Physiol.*, 49 (10): 1614-20.

Shimmen, T., Kikuyama, M., Tazawa, M. (1976). Demonstration of two stable potential states of plasmalemma of *Chara* without tonoplast. *J. Membr. Biol.*, 30: 249-70.

Shimmen, T., Mimura, T., Kikuyama, M., Tazawa, M. (1994). Characean cells as a tool for studying electrophysiological characteristics of plant cells. *Cell Struct. Funct.*, 19: 263-78.

Sun, J., Qi, L., Li, Y., Zhai, Q., Li, C. (2013). PIF4 and PIF5 transcription factors link blue light and auxin to regulate the phototropic response in Arabidopsis. *The Plant Cell*, 25: 2102-14.

Takahashi, K., Hyashi, K., Kinoshita, T. (2012). Auxin activates the plasma membrane H^+-ATPase by phosphorylation during hypocotyl elongation in Arabidopsis. *Plant Physiol.*, 159: 32-641.

Tarakhovskaya, E.R., Maslov, Y.I., Shishova, M.F. (2007). Phytohormones in algae. *Russ. J. Plant Physiol.*, 54: 163-70.

Tatematsu, K., Kumagai, S., Muto, H., Sato, A., Watahiki, M., Harper, R.M. Liscum, E., Yamamoto, K.T. (2004). MASSUGU2 encodes Aux/IAA19, an auxin-regulated protein that functions together with the transcriptional activator NPH4/ARF7 to regulate differential growth responses of hypocotyl and formation of lateral roots in Arabidopsis thaliana. *The Plant Cell*, 16: 379-93.

Tazawa, M. and Shimmen, T. (2001). How characean cells have contributed to the progress of plant membrane biophysics. *Aust. J. Plant Physiol.*, 28: 523-39.

Tsutsui, I. and Ohkawa, T. (2001). Regulation of the H^+ pump activity in the plasma membrane of internally perfused *Chara coralline. Plant Cell Physiol.*, 42 (5): 531-7.

Timme, R.E., Bachvaroff, T.R., Delwiche, C.F. (2012). Broad phylogenomic sampling and the sister lineage of land plants. *PLoS One*, 7 (1): e29696. doi:10.1371/journal.pone.0029696.

Van Duijn, B. and Heimovaara-Dijkstra, S. (1994). Intracellular microelectrode membrane potential measurements in tobacco cell-suspension protoplasts and barley aleurone protoplasts: interpretation and artifacts. *Biochim. Biophys. Acta.*, 1193: 77-84.

Van Overbeek, J. (1940). Auxin in marine algae. *Plant Physiol.*, 15: 291-9.

Vernoux, T., Besnard, F., Traas, J. (2010). Auxin at the shoot apical meristem. *Cold Spring Harb. Perspect. Biol.*, 2: a001487

Viaene, T., Delwiche, C.F., Rensing, S.A., Friml, J. (2013). Origin and evolution of PIN auxin transporters in the green lineage. *Trends Plant Sci.*, 18: 5-10.

Viaene, T., Landberg, K., Thelander, M., Medvecka, E., Pederson, E., Feraru, E. Cooper, E.D., Karimi, M., Delwiche, D.F., Ljung, K., Geisler, M., Sundberg,E., Friml, J. (2014). Directional auxin transport mechanisms in early diverging land plants. *Curr. Biol.*, 24 (23): 2786-91. doi: 10.1016/j.cub.2014.09.056.

Wodniok, S., Brinkmann, H., Glockner, G., Heidel, A.J., Philippe, H., Melkonian, M., Becker, B. (2011). Origin of land plants: do conjugating green algae hold the key? *BMC Evol. Biol.*, 11: e104.

Wright, R.C. and Nemhauser, J.L. (2015). New tangles in the auxin signaling web. *F1000Prime Rep.*, 7: 19. doi:10.12703/P7-19

Xu, W., Jia, L., Shi, W., Liang, J., Zhou, F., Li, Q., Zhang, J. (2012). Abscisic acid accumulation modulates auxin transport in the root tip to enhance proton secretion for maintaining root growth under moderate water stress. *New Phytol.*, 197: 139-50. doi: 10.1111/nph.12004

Zhang, S. and van Duijn, B. (2014). Cellular auxin transport in algae. *Plants*, 3: 58-69.